# Successive Successful Uplinks-Based Reliability Analysis for Satellite-IoT Networks

Ayush Kumar Dwivedi<sup>®</sup>, Fatemeh Rafiei Maleki, and Taneli Riihonen<sup>®</sup>
Faculty of Information Technology and Communication Sciences, Tampere University, Finland
email: ayush.dwivedi@tuni.fi

Abstract—Internet-of-Things (IoT) devices often communicate with burst periodic transmissions. This paper studies the reliability of such burst transmissions in low Earth orbit (LEO) satellite-based IoT networks under a block-ALOHA random access protocol. Devices associate with the nearest visible satellite, and the link is modeled with realistic shadowed-Rician fading and stochastic geometry for satellite positions. A deadline-constrained reliability metric that accounts for "successive successful uplinks" within a defined block of time is used. Theoretical analysis and Monte-Carlo simulations provide design-oriented guidance for selecting MAC and PHY parameters in satellite IoT systems.

Index Terms—IoT networks, LEO satellites, reliability analysis, stochastic geometry

### I. Introduction

Low Earth orbit (LEO) satellites can provide seamless connectivity to Internet-of-Things (IoT) networks deployed over large geographical areas [1]. IoT traffic is often short, sporadic, and bursty: sensors send small reports on alarms, meter reads, or environmental events. These reports must be delivered quickly and reliably. Grant-free uplinks address this by sending multiple replicas in a short burst so the receiver can lock in frequency/time under Doppler, perform combining, and pass a cyclic redundancy check [2]. This creates a run-length requirement: the receiver needs a streak of successful decoding events over successive slots within one access attempt. This becomes challenging in LEO satellite links because of large path loss, strong Doppler, time visibility, moving beams, and contention from many devices within a wide footprint. Therefore, a model incorporating satellite geometry, random access (RA), and fading environment is required to design and analyze networks for reliable satellite-IoT communication.

This work is inspired by the "statistics of successive successful detection" concept developed for radar tracking [3]. The author in [3] analyzed the probability that an automotive radar produces consecutive detections within a time budget. We adapt that run-length viewpoint to LEO uplinks for IoT communication. We conceptualize a reliable block of uplinks to occur when at least a specified number of messages are decoded consecutively during one access attempt. Similarly, a delivery window is considered reliable if at least one reliable block occurs before the latency deadline of the IoT application. At the same time, a frame-slotted ALOHA captures access

This research work was supported partly by Business Finland through the project "Stochastic 3D Modelling of 6G Networks" and partly by the Research Council of Finland under the grant #367805.

with a duty cycle and a finite set of orthogonal preambles. This definition aligns with ultra-reliable low latency communication (URLLC) practice, where reliability is the probability that a report is delivered within its deadline.

Several prior works relate to parts of the problem studied in this paper. The radar signal processing, wireless communication, and coding theory communities have long studied run-length or m-of-n confirmation logic. For example, the work in [4] analyzes a radar detection scheme that requires m consecutive pulse detections out of n pulses, modeling the detection process as a Markov chain. In [5], the authors introduced a conditional packet delivery function representing the probability that the next packet succeeds given a run of n consecutive successes (or failures) preceding it. It is used to quantify link burstiness and adapt sensor-network protocols to reduce average transmission cost. Similarly, [6] developed streaming codes that enable recovery within a decoding window for channels with bursts/runs of erasures. However, such concepts of run length have been less explored in the context of satellite communication.

This paper focuses on creating a tractable framework by translating the consecutive-success reliability metric to LEO satellite-IoT and connecting it to stochastic geometry and random access. Recently, a few studies for LEO satellite systems have used stochastic geometry to analyze coverage [7]–[9], and meta-distributions [10] under various satellite-association policies. Topologies and transmission schemes for satellite-IoT have also been analyzed using stochastic geometry in [11], [12]. However, these works typically decouple MAC from the geometry, in contrast to the approach taken in this paper. Time-related reliability has also been explored for URLLC in [13], and for repetition-based grant-free access in [14], [15], but for a terrestrial setting only.

In this paper, we propose the concept of a satellite-IoT network with nearest-satellite association, block-ALOHA random access, and a shadowed-Rician fading environment. The delivery window-constrained reliability metric for the proposed concept is defined based on successive successful uplinks. We derive expressions for per-block and within-delivery-window reliability and validate them using Monte Carlo simulations. The numerical results provide design insights on how reliability varies with channel access parameters, the number of RA preambles, narrowband operation supports longer run-lengths, and constellation size and altitude interact with latency.

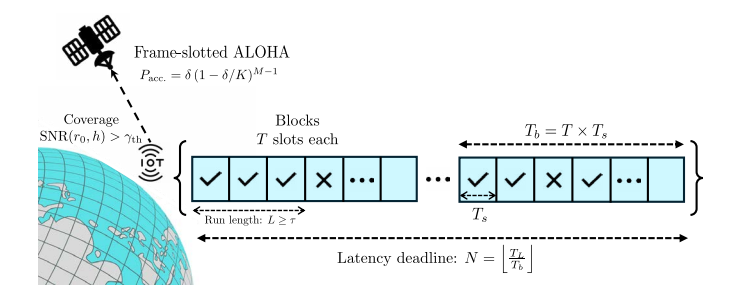


Fig. 1. LEO satellite-IoT uplink with frame-slotted ALOHA. A block of T slots is "reliable" if per-slot SNR exceeds threshold for  $\tau$  consecutive slots; a packet meets the latency target if one reliable block occurs within N blocks.

### II. SYSTEM MODEL

Consider a satellite-based IoT network consisting of multiple IoT devices on Earth's surface attempting to communicate with a constellation of LEO satellites. The devices communicate their sensed information using a block-ALOHA-based random access protocol to the nearest satellite whose location is modeled using stochastic geometry. Fig. 1 shows the system concept studied in this paper.

### A. Spatial Distribution of Satellites

Consider S LEO satellites distributed randomly and uniformly on a spherical shell at an altitude  $r_{\min}$  above the Earth's surface, forming a binomial point process (BPP)  $\Phi$  on a sphere. The Earth's radius is denoted by  $r_E$ ; thus, the satellite orbital radius is  $r_{\min} + r_E$ . As given in [11], the probability distribution function (pdf),  $f_R(r)$ , of the distance between a satellite and an arbitrary device on Earth's surface is

$$f_R(r) = \frac{2r}{r_{\text{max}}^2 - r_{\text{min}}^2},\tag{1}$$

for  $r_{\min} \leq r \leq r_{\max}$ , and  $f_R(r) = 0$  otherwise. Here  $r_{\max} = \sqrt{(r_E \sin \theta_0)^2 + (r_E + r_{\min})^2 - r_E^2} - r_E \sin \theta_0$  is the maximum distance observed at the mask elevation angle  $\theta_0$ . Moreover, the number of satellites visible with an elevation angle greater than the mask angle would be a binomial random variable with success probability given in [11] as

$$p_{\text{vis}} = \frac{r_{\text{max}}^2 - r_{\text{min}}^2}{4 r_E \left( r_E + r_{\text{min}} \right)}.$$
 (2)

## B. Signal and Channel Model

Each packet transmission experiences independent channel conditions across different slots. The devices are assumed to connect to the nearest visible satellite in the constellation at a distance  $r_0$ . The uplink channel from the IoT device to the satellite is modeled as a shadowed-Rician fading channel. Specifically, the signal-to-noise ratio (SNR) for each transmission is given by

$$SNR(R_0, h) = \frac{P_t \cdot G_t \cdot G_r}{N_0 B} \cdot |h|^2 \left(\frac{\lambda}{4\pi R_0}\right)^2, \quad (3)$$

where  $P_t$  is the transmitting power of the IoT device,  $G_t$  and  $G_r$  represent the transmit and receive antenna gains, h is the

complex fading coefficient,  $N_0$  is the noise spectral density,  $\lambda$  is the wavelength corresponding to the carrier frequency  $f_c$ , and B is the system bandwidth.

**Definition** 1 (Successful uplink): We define a transmission within a slot as successful with the device under coverage if the instantaneous SNR exceeds a predefined threshold  $\gamma_{\rm th}$ . Therefore, the conditional coverage probability of a device, given that it is connected to the nearest visible satellite in an instance of  $\Phi$ , is given by

$$P_{c} = \Pr[SNR(r_{0}, h) > \gamma_{th} \mid \Phi]$$

$$= \overline{F}_{H}(r_{0}^{2} \gamma_{th}), \tag{4}$$

where  $\overline{F}_H(h)$  denotes the complementary cdf (CCDF) of a weighted squared Shadowed-Rician fading amplitude,  $H = \eta |h|^2$  as given in [11, Eq. 3].

#### C. Block ALOHA-based Random Access Protocol

Let M denote the number of IoT devices within the coverage region, each independently attempting to access satellite resources following a block-based RA scheme. Specifically, the time is divided into blocks of duration  $T_b$  seconds. We employ a frame-slotted ALOHA-style random access with K contention mini-slots/preambles: each IoT device independently contends for the resource by picking one of K preambles uniformly at random with a duty cycle parameter  $\delta \in [0,1]$ , i.e., the probability with which each IoT device independently attempts to access a given block.

A device acquires a resource and attempts uplink transmission in a given block if it is the only device using its chosen preamble, i.e., *K* winners per block, on orthogonal resources. If multiple devices choose the same preamble, a collision occurs, and no device transmits. Upon collision, devices perform an independent random back-off before their next attempt. Consequently, the probability of successful resource acquisition (collision-free access) for a device is given by

$$p_{\text{access}} = \delta \left( 1 - \delta / K \right)^{M-1}. \tag{5}$$

The connected IoT device transmits T consecutive packets during that block upon successful acquisition. Each block is further segmented into T slots, each duration  $T_s$ , such that  $T_b = T \times T_s$ . We assume the satellite geometry (i.e., satellite positions) remains fixed within each block duration, since the relative movements of typical LEO satellites over short intervals (a few hundred milliseconds) are negligible.

Let  $L \in [0,T]$  be the random variable representing the maximum run length of the uplink successes in a block for the IoT device, i.e., the device experiences L consecutive successful receptions at the satellite. However, note that the device does not necessarily get to use every block since a per-block access success probability exists.

**Definition** 2 (Reliable block and window): We define a single block of T uplinks as reliable if the satellite successfully receives the packet in  $\tau$  consecutive slots, i.e., the event  $L \geq \tau$ , for some  $\tau \leq T$ . Similarly, we define a delivery window to be end-to-end reliable, if a reliable block is obtained within a latency deadline of N blocks (i.e., retries).

#### III. STATISTICS OF RELIABILITY

The distance distribution to the nearest visible satellite and the moments of conditional coverage probability would be required to find the statistics of end-to-end reliability averaged over the satellite realizations.

1) Distance distribution to the nearest visible satellite: The pdf of the slant range between an IoT device and a satellite in the visibility region is given by (1). Using order statistics, the unconditional pdf of the distance to the nearest visible satellite can be written as

$$f_{R_0}(r) = S p_{\text{vis}} f_R(r) (1 - p_{\text{vis}} F_R(r))^{S-1}$$
. (6)

Therefore, the pdf  $f_{R_0}(r)$  conditioned on there being at least one visible satellite can be written as

$$f_{R_0|S_{\text{vis}} \ge 1}(r) = \frac{S p_{\text{vis}} f_R(r) (1 - p_{\text{vis}} F_R(r))^{S-1}}{1 - (1 - p_{\text{vis}})^S}.$$
 (7)

2) Moment of the conditional coverage: The moments of the conditional coverage probability  $P_c$  within a block for a device connecting to the nearest visible satellite are given by

$$\zeta(t) = \mathbb{E}[P_{c}^{t}] 
= \frac{S p_{\text{vis}}}{1 - (1 - p_{\text{vis}})^{S}} \int_{r_{\text{min}}}^{r_{\text{max}}} (\overline{F}_{H}(r_{0}^{2} \gamma_{\text{th}}))^{t} f_{R}(r_{0}) 
\times (1 - p_{\text{vis}} F_{R}(r_{0}))^{S-1} dr_{0}.$$
(8)

3) Probability of reliable block and window: For a given realization of satellite locations  $\Phi$  and provided that an IoT device acquires access to the nearest satellite, the conditional CCDF  $F_L(\tau) = \Pr[L \geq \tau \mid \Phi]$  of L as a function of  $P_c$  can be characterized using the *de Moivre's solution* for run length probability given in [16, Section 22.6] as

$$F_L(\tau) = \sum_{l=1}^{\lfloor \frac{T+1}{\tau+1} \rfloor} (-1)^{l+1} \left( P_c + \frac{T - l\tau + 1}{l} (1 - P_c) \right) \times {T - l\tau \choose l - 1} P_c^{l\tau} (1 - P_c)^{l-1}.$$
(9)

The first moment of this conditional CCDF of the block length gives the probability of having a single reliable block as

$$P_{\rm r}(\tau;T) = \mathbb{E}\left[F_L(\tau)\right] = \sum_{l=1}^{\lfloor \frac{T+1}{\tau+1} \rfloor} (-1)^{l+1} \binom{T-l\tau}{l-1} \times \mathbb{E}\left[\frac{T-l\tau+1}{l}P_{\rm c}^{l\tau}\left(1-P_{\rm c}\right)^l + P_{\rm c}^{l\tau+1}\left(1-P_{\rm c}\right)^{l-1}\right].$$
(10)

Using binomial expansion to expand the power terms, and substituting (8) in (10) gives

$$P_{r}(\tau;T) = \sum_{l=1}^{\lfloor \frac{T+1}{\tau+1} \rfloor} (-1)^{l+1} {T - l\tau \choose l-1} \times \left( \sum_{\ell=0}^{l-1} {l-1 \choose \ell} (-1)^{\ell} \zeta(l\tau + 1 + \ell) + \frac{T - l\tau + 1}{l} \sum_{\ell=0}^{l} {l \choose \ell} (-1)^{\ell} \zeta(l\tau + \ell) \right). \quad (11)$$

Finally, the end-to-end reliability within a delivery window, i.e., probability that a packet from the device is delivered (i.e., achieves at least one successive successful uplink-qualified block) within the latency deadline, can be written as

$$P_{\rm r}(\tau; T, N) = 1 - (1 - p_{\rm access} P_{\rm r}(\tau; T))^{N}.$$
 (12)

## IV. NUMERICAL RESULTS

In this section, we corroborate the theoretical analysis with the Monte-Carlo simulations and present some useful insights for system design. We model the load per beam, i.e., the number of IoT devices (M) attempting to access satellite resources in a block, based on the beam footprint and terminal density. Consider that the LEO satellite generates a circular spot beam with diameter  $d_{\text{beam}}$  and area  $A_{\text{beam}}$ . We assume narrow LEO spot beams such that the IoT devices are modeled (using a standard planar approximation) as a homogeneous Poisson Point Process with density  $\lambda_d$  (devices/km²), and arrival rate  $\mu$  (per second per device). Therefore, the probability that a device has at least one packet to transmit during the block is  $p_{\text{traffic}} = 1 - \exp(-\mu T_b)$ . Based on the above modeling, the mean number of contending devices can be obtained as

$$M = \lambda_d A_{\text{beam}} p_{\text{traffic}}.$$
 (13)

To compute the end-to-end reliability obtained with retries over N blocks in a delivery window, we consider a latency deadline  $T_L$  such that

$$N = \left| \frac{T_L}{T_h} \right| . \tag{14}$$

This latency deadline  $T_L$  sets how many access blocks a device can try before the packet is late/dropped. For the LEO satellite, it also aligns with short visibility windows, faster handovers, and application timeliness (e.g., alarms vs. telemetry). Hence, it is an essential quality-of-service (QoS) parameter.

Following the description on IoT support for non terrestrial networks in [2], we use the following parameters for simulations unless specified otherwise:  $P_t=26$  dBm,  $G_t=0$  dBi,  $G_r=30$  dBi, B=15 kHz (i.e., single-tone narrowband IoT),  $f_c=2$  GHz,  $\gamma_{\rm th}=-10$  dB,  $r_E=6371$  km,  $r_{\rm min}=600$  km,  $\theta_0=10^\circ$ , and S=720. The channel between the IoT devices and the satellites is assumed to be average shadowed with parameters as mentioned in [11]. For simulating the successive uplinks within the delivery window, we use  $T_b=200$  ms,  $T_s=10$  ms,  $T_L=5$  s,  $d_{\rm beam}=550$  km,

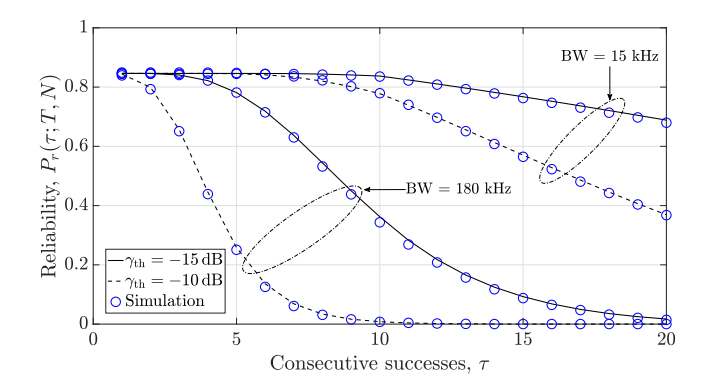


Fig. 2. Impact of the PHY strength  $(\gamma_{\rm th}, B)$  on reliability w.r.t. consecutive successes,  $\tau$  (here T=20 slots, K=5,  $\delta=K/M$ , and  $\lambda_{\rm d}=1/{\rm km}^2$ ).

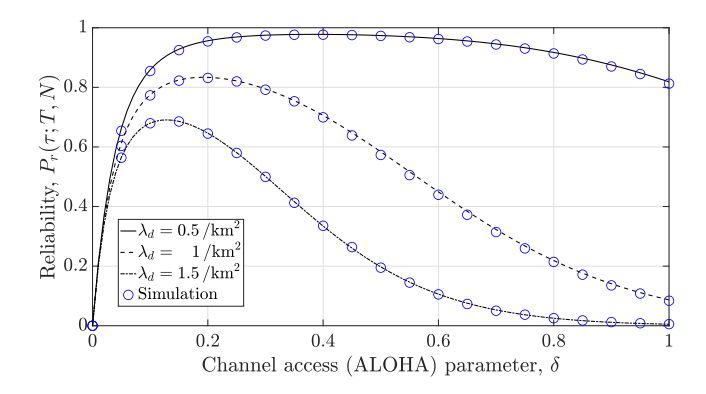


Fig. 3. Impact of the device deployment density on reliability w.r.t. the channel access parameter (here T=20 slots,  $\tau=7$ , and K=5).

 $\mu=2$  messages per hour, and K=5 preambles. The tight match between simulation (markers) and theory (lines) in the following plots verifies the presented theoretical model under shadowed-Rician fading and the slot-i.i.d. assumption.

Fig. 2 shows the end-to-end reliability  $P_{\rm r}(\tau;T,N)$  w.r.t. number of constitutive success  $(\tau)$  required for a reliable block. With the MAC fixed at its near-optimum  $\delta = K/M$ , reliability is driven entirely by the within-block successive successful uplink term  $P_{\rm r}(\tau;T)$  given in (11). Since  $P_{\rm r}$  is the CCDF of the longest success run in T i.i.d. Bernoulli trials with per-slot success  $P_c$ , it decays rapidly with an increase in  $\tau$ . The two PHY parameters that affect  $P_c$  are analyzed in this figure. Tightening the SNR threshold lowers  $P_c$  and steepens the drop, while increasing bandwidth raises the noise floor  $(N_0B)$ , producing the same qualitative effect. It can be observed that for  $\gamma_{\rm th} = -10$  dB at 180 kHz, the reliability collapses around  $\tau \approx 8-10$ , whereas at 15 kHz (a much narrower tone) the curve remains high out to much larger  $\tau$ . However, at  $\gamma_{\rm th} = -15$ , both bandwidths sustain larger  $\tau$ , with the 15 kHz case showing the slowest decay.

It can be inferred that for satellite-based IoT, narrowband modes (e.g., 3GPP NTN/NB-IoT single-tone) or equivalent combining gains are essential if applications demand long consecutive success streaks. Even modest PHY margin changes result in order-of-magnitude shifts in  $P_{\rm r}$  because the run-length probability is exponentially sensitive to the per-slot success  $P_c$ .

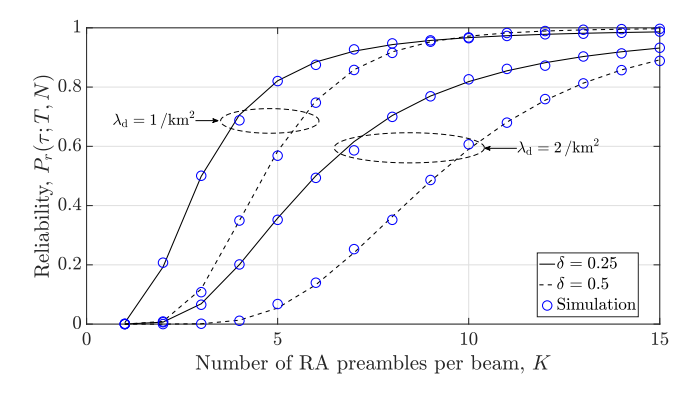


Fig. 4. Impact of access parameter  $\delta$ , and deployment density on reliability w.r.t. the no. of RA preambles per beam, K (here T=20 slots, and  $\tau=7$ ).

Choosing  $\tau$  relates to service tiers of the IoT application. A small  $\tau$  is suitable for lightweight sensing, whereas a larger  $\tau$  is required for more robust uploads. Careful selection ensures a robust burst under real LEO impairments (viz. Doppler and timing uncertainty) and supports HARQ/repetition combining.

Fig. 3 shows the end-to-end reliability w.r.t. the channel access parameter  $\delta$ . Here, the within-block reliability,  $P_{\rm r}(\tau;T)$ , is fixed across curves, and the device deployment density  $\lambda_d$ controls the access probability  $p_{\text{access}}$ . The shape of the curves represents the classic ALOHA trade-off. However, the device deployment density differentiates the right-tail behavior. For  $\lambda_d = 0.5/\mathrm{km}^2$  (a sparse deployment scenario), the curve does not fall to zero—it bottoms out around  $\delta = 0.8$ . This is because in the multi-preamble RA model, the per-device access even at  $\delta = 1$  is  $(1 - 1/K)^{M-1}$ . It is sizable when M is comparable to K, meaning many blocks still yield singleton preambles. In contrast, for denser deployments ( $\lambda_d = 1$  and  $1.5/\mathrm{km}^2$ ),  $M \gg K$  and  $p_{\mathrm{access}}$  decays rapidly, and hence the reliability approaches zero on the right. An optimal channel access parameter is important to maintain device energy use and regulatory duty-cycle limits. It also helps avoid access collapse during peak visibility and maintain smooth load across a satellite pass.

Fig. 4 shows the reliability with increasing number of RA preambles (K) for varying device deployment density  $\lambda_d$  and channel access parameter ( $\delta$ ). When K is small, the effective load per preamble is high, leading to a low reliability ( $p_{access}$  is significantly less). As K increases, the effective load decreases and reliability increases. The rise is much faster for lower  $\lambda_d$ , since lower M yields a lighter effective load per preamble. All curves saturate for large K at the collision-free ceiling 1- $(1-\delta P_r(\tau;T))^N$  (since  $(1-\delta/K)^{M-1}\to 1$ ), which explains why higher  $\delta$  ultimately attains higher asymptote (visible for  $\lambda_d = 1$  case at the top right corner of the plot). However, at moderate K values, the lower channel access parameters can perform better because they suppress collisions. To maintain a given reliability, K must scale roughly linearly with M as a design rule for selecting the size of the preambles per beam. However, with high Doppler and timing offsets, only a limited set of orthogonal preambles is practical in satellite-IoT.

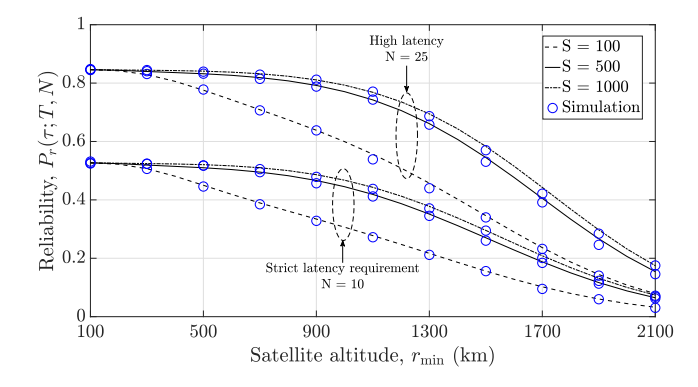


Fig. 5. Impact of satellite scenario (no. of satellites, S) and latency requirements (tied with N) on reliability w.r.t. satellite altitude,  $r_{\min}$ .

Fig. 5 shows the reliability w.r.t. the constellation parameters like satellite altitude, number of satellites in the constellation, and the latency requirement. Reliability drops with altitude as the slant range and path loss grow, reducing perslot success. Adding satellites to the constellation helps by tightening the nearest-satellite distance distribution, but the gain saturates once the geometry is already "dense enough" and contention/altitude dominate. An increase in the latency deadline increases the reliability, with more benefit at higher altitudes where per-block reliability is small. It can be observed that when the constellation size is beyond the sparse regime, we can trade between S and N depending on whether CAPEX (satellites) or QoS (latency) is the tighter constraint.

## V. CONCLUSION

This paper analyzed the reliability in satellite-IoT networks, capturing MAC access and the probability of achieving the required successive successful uplinks within a block. We demonstrated how reliability can be engineered by tuning the duty cycle and preambles to the traffic load, exploiting narrowband operation, selecting an adequate constellation size, and budgeting sufficient blocks within the latency deadline. In the future, a more comprehensive study with interference from other devices that grows with the access parameter (beyond the collision-only model) and meta-distribution of the successive successes (capturing user-to-user variability) can be explored.

#### REFERENCES

- [1] S. Kota et al., "INGR roadmap satellite chapter," in 2023 IEEE Future Networks World Forum (FNWF), 2023, pp. 1–195.
- [2] 3rd Generation Partnership Project (3GPP); Technical Specification Group Radio Access Network, "Study on NB-IoT/eMTC support for Non-Terrestrial Networks (NTN) (Rel 17)," TR 36.763V17.0.0, 2021.
- [3] G. Ghatak, "Target tracking: Statistics of successive successful target detection in automotive radar networks," arXiv preprint arXiv:2411.18252, 2024
- [4] M. Bell, "Contiguous pulse binary integration analysis," *IEEE Transactions on Aerospace and Electronic Systems*, vol. 32, no. 3, pp. 923–933, 1996.
- [5] K. Srinivasan, M. A. Kazandjieva, S. Agarwal, and P. Levis, "The β-factor: Measuring wireless link burstiness," in *Proceedings of the 6th ACM Conference on Embedded Network Sensor Systems*, ser. SenSys '08, 2008, p. 29–42.
- [6] S. L. Fong, A. Khisti, B. Li, W.-T. Tan, X. Zhu, and J. Apostolopoulos, "Optimal streaming codes for channels with burst and arbitrary erasures," in 2018 IEEE International Symposium on Information Theory (ISIT), 2018, pp. 1370–1374.
- [7] N. Okati, T. Riihonen, D. Korpi, I. Angervuori, and R. Wichman, "Downlink coverage and rate analysis of low Earth orbit satellite constellations using stochastic geometry," *IEEE Transactions on Communications*, vol. 68, no. 8, pp. 5120–5134, 2020.
- [8] N. Okati and T. Riihonen, "Nonhomogeneous stochastic geometry analysis of massive LEO communication constellations," *IEEE Transactions* on *Communications*, vol. 70, no. 3, pp. 1848–1860, 2022.
- [9] —, "Stochastic coverage analysis for multi-altitude LEO satellite networks," *IEEE Communications Letters*, vol. 27, no. 12, pp. 3305– 3309, 2023.
- [10] B. Naganjani, A. K. Dwivedi, S. Chaudhari, and T. Riihonen, "Analyzing 6G satellite IoT architecture using stochastic geometry: A meta distribution approach," in 2024 IEEE Globecom Workshops (GC Wkshps), 2024, pp. 1–6.
- [11] A. K. Dwivedi, S. Chaudhari, N. Varshney, and P. K. Varshney, "Performance analysis of LEO satellite-based IoT networks in the presence of interference," *IEEE Internet of Things Journal*, pp. 1–1, 2023.
- [12] A. K. Dwivedi, H. Chougrani, S. Chaudhari, N. Varshney, and S. Chatzinotas, "Efficient transmission scheme for LEO satellite-based NB-IoT: A data-driven perspective," arXiv preprint arXiv:2406.14107, 2024.
- [13] T. Hößler, M. Simsek, and G. P. Fettweis, "Mission reliability for URLLC in wireless networks," *IEEE Communications Letters*, vol. 22, no. 11, pp. 2350–2353, 2018.
- [14] G. Berardinelli et al., "Reliability analysis of uplink grant-free transmission over shared resources," *IEEE Access*, vol. 6, pp. 23 602–23 611, 2018
- [15] T. Jacobsen, R. Abreu, G. Berardinelli, K. Pedersen, I. Z. Kovacs, and P. Mogensen, "System level analysis of k-repetition for uplink grant-free URLLC in 5G NR," in 25th European Wireless Conference, 2019, pp. 1–5.
- [16] A. Hald, A history of probability and statistics and their applications before 1750. John Wiley & Sons, 2005.